Robust design of Si/Si$_3$N$_4$ high contrast grating mirror for mid-infrared VCSEL application

C. Chevallier · N. Fressengeas · F. Genty · J. Jacquet

Abstract   A Si/Si$_3$N$_4$ high contrast grating mirror has been designed for a VCSEL integration in mid-infrared ($\lambda = 2.65\,\mu$m). The use of an optimization algorithm which maximizes a VCSEL mirror quality factor allowed the adjustment of the grating parameters while keeping large and shallow grating pattern. The robustness with respect to fabrication error has been enhanced thanks to a precise study of the grating dimension tolerances. The final mirror exhibits large high reflectivity bandwidth with a polarization selectivity and several percent of tolerance on the grating dimensions.

Keywords   High contrast grating mirror · Mid-infrared VCSEL · Robust design

1 Introduction

High contrast grating (HCG) mirrors with a grating period smaller or in the range of the reflected wavelength can be designed to exhibit very high performances with energy only in the 0-order of diffraction. HCGs which are made of a high index grating on top of a low index sublayer can achieve a reflectivity as high as 99.9 % and bandwidths larger than 100 nm together with a strong polarization selectivity between TM and TE mode (Mateus et al. 2004; Chevallier et al. 2011). These characteristics are very interesting for replacing the top Bragg mirror in VCSEL devices (Huang et al. 2007). Moreover, the circular VCSEL structure usually presents no polarisation selectivity and the use of a grating should improve the stability of the emitted beam (Debernardi et al. 2005). Also, the wavelength of emission of mid-IR electrically-pumped VCSEL is currently limited close to 2.6 μm since the necessary semiconductor Bragg mirrors become as thick as 11 μm with more than 20 quarter wavelength

C. Chevallier (✉) · F. Genty · J. Jacquet
Supélec, 2 rue Edouard Belin, 57070 Metz, France
e-mail: christyves.chevallier@supelec.fr

N. Fressengeas
LMOPS, Laboratoire Matériaux Optiques, Photonique et Systèmes, EA 4423, Unité de Recherche Commune à l'Université Paul Verlaine, Metz et Supélec, 2 rue Edouard Belin, 57070 Metz, France

Fig. 1 Scheme of the HCG optimized for $\lambda_0 = 2.65\,\mu m$ exhibiting a 218 nm large bandwidth with $L_e = 829\,nm$, $L_f = 522\,nm$, $T_g = 899\,nm$, $T_L = 896\,nm$
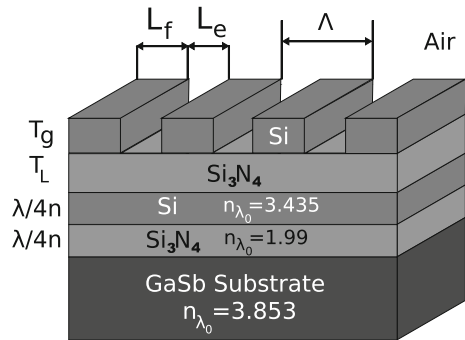
pairs (Ducanchez et al. 2009; Bachmann et al. 2009) making the epitaxial growth control critical. With a reduction of a factor of 5 of the thickness of the top mirror and fabrication tolerances as large as 20 % (Zhou et al. 2008; Chevallier et al. 2012), the use of HCGs should allow VCSEL operation at larger wavelengths. Moreover, the HCG dimensions are scalable with the wavelength in the limit of the refractive index dispersion (Mateus et al. 2004) which makes the designs presented in this work scalable for other wavelengths.

In this work, we design a Si/Si₃N₄ HCG for a VCSEL application at 2.65 μm. First, the optical properties that VCSEL mirrors must exhibit are defined and quantitatively expressed through a quality factor. The dimensions of the HCG structure are then adjusted by an optimization algorithm to maximize the quality factor and meet VCSEL requirements. Finally, the HCG robustness is enhanced through a precise study of the tolerance on the physical dimensions. The final design has thus an optimized reflectivity with several percent of tolerance as an error margin that the technological manufacturing process must respect.

2 Mirror design

In a previous works (Chevallier et al. 2012), Si/SiO₂ structures were designed for applications at $\lambda = 2.65\,\mu m$. However in the 2.65–3 μm wavelength range, OH-radicals present an absorption band (Soref et al. 2006) and could decrease the HCG performances depending on their concentration in the SiO₂ layer (Chevallier et al. 2012). The Si₃N₄ should be well suitable for the low index material since it exhibits no absorption at these wavelengths (Soref et al. 2006). The mirror structure presented in Fig. 1 is made of a silicium grating ($n = 3.435$) on top of a Si₃N₄ layer as the low index sublayer ($n = 1.99$). A Si/Si₃N₄ quarter wavelength pair has been added below the HCG in order to increase the width of the reflectivity bandwidth (Chevallier et al. 2011). The mirror structure has thus several dimension lengths to define: the etched length L_e, the filled length L_f, the grating thickness T_g and the sublayer thickness T_L. Contrary to Bragg mirrors, HCG design rules to achieve high reflectivity are not straightforward and require an optimization process to match the expected properties.

The VCSEL application requires specific properties on the optical performances of the mirror in order to create a cavity of sufficient quality for laser emission. Due to the thin gain region of the VCSEL structure, the reflectivity of the mirror is typically chosen to be as high as 99.5 % for the largest possible bandwidth. However, a 99.9 % reflectivity threshold has been chosen to ensure a fabrication security margin. Moreover, due to their one dimensional symmetry, HCG can be shaped to obtain a polarization selectivity. Thus, the reflectivity threshold of 99.9 % is applied only for transverse magnetic (TM) mode while keeping a

transverse electric (TE) reflectivity below 90 %, so that the laser effect should be possible only in TM polarization.

The mirror is simulated by the rigorous coupled wave analysis (RCWA) method (Moharam et al. 1995; Rathgen 2010) which computes reflection spectra for TM and TE modes for perfectly squared grating with an infinite number of periods. Calculations were done by using constant index values.

Through a numerical analysis of the computed reflection spectra, the quality of a design is quantitatively evaluated by the use of a quality factor Q (Chevallier et al. 2011):

$$Q = \frac{\Delta\lambda}{\lambda_0} \frac{1}{N} \sum_{\lambda=\lambda_1}^{\lambda_2} R_{TM}(\lambda) g(\lambda) \tag{1}$$

This quality factor is written to take into account the previously defined VCSEL requirements with a polarization selectivity performed by selecting the range of wavelengths $\Delta\lambda$ around λ_0 for which R_{TM} is higher than 99.9 % and R_{TE} is lower than 90 %. This selection starts at the aimed wavelength λ_0 and is enlarged both for larger and smaller wavelengths around λ_0 while the reflection conditions are met giving two boundaries: λ_1 and λ_2. The centering of the bandwidth around $\lambda_0 = 2.65\,\mu$m is made by computing a gaussian weighted average of the R_{TM} values on the N points of the bandwidth $[\lambda_1, \lambda_2]$. Finally the influence of the width of the stopband is expressed in this quality factor by multiplying the latter average by the bandwidth itself $\Delta\lambda = |\lambda_2 - \lambda_1|$ and normalized by λ_0.

3 Optimization

The optimization of the mirror performance is made by adjusting the grating parameters to maximize the quality factor Q. However, with its numerous local maxima, its non linearity and unknown derivative, this Q factor can only be optimized using a global maximization method. The Differential Evolution algorithm (Kroshko 2009; Feoktistov 2006) has been used as optimization algorithm to find automatically the best set of parameters which maximizes the mirror quality.

The Si/Si$_3$N$_4$-based structure presented in Fig. 1 has been optimized under constraints by using large and shallow grooves (L_f, $L_e > 500$ nm and an aspect ratio $T_g/L_e < 1.1$). These limitations are relatively severe for the optimization algorithm since the Si/SiO$_2$ HCGs are typically defined with narrower patterns of less than 260 nm and large aspect ratio of more than 2.6 (Mateus et al. 2004). Since HCGs require a vertical etching profile with squared pattern to reach the 99.9 % high reflectivity, the technological constraints were chosen to obtain an experimental square grating profile as close as possible to the theoretical one. However, these values can be easily adjusted before the optimization by the manufacturers according to the etching process used and the machine specifications.

The resulting optimum grating parameters (Table 1) are $L_e = 829$ nm, $L_f = 522$ nm, $T_g = 899$ nm, $T_L = 896$ nm. This mirror design exhibits a 218 nm large bandwidth with $R_{TM} > 99.9\%$ together with a high polarization selectivity by keeping $R_{TE} < 90\%$ and meets all previously defined VCSEL requirements.

In order to evaluate the feasibility of the design, a tolerance study has been performed on the dimensions of the grating. The tolerance of one parameter is defined as the allowed variation range of this parameter for which the mirror is performant enough for a VCSEL application with $R_{TM} > 99.9\%$ and $R_{TE} < 90\%$. From a fabrication point of view, the most critical parameters of the grating are the etched length L_e and the filled length L_f which result

Table 1 Dimensions and tolerances of the optimum mirror

Parameter	Optimum	Minimum	Maximum	Tolerance
L_e	829 nm	763 nm	831 nm	$\pm 0.2\,\%$
L_f	522 nm	498 nm	522 nm	$\pm 0\,\%$
T_g	899 nm	897 nm	941 nm	$\pm 0.2\,\%$
T_L	896 nm	806 nm	976 nm	$\pm 8.9\,\%$
$\Delta\lambda$	218 nm			
$\Delta\lambda/\lambda_0$	8.3 %			
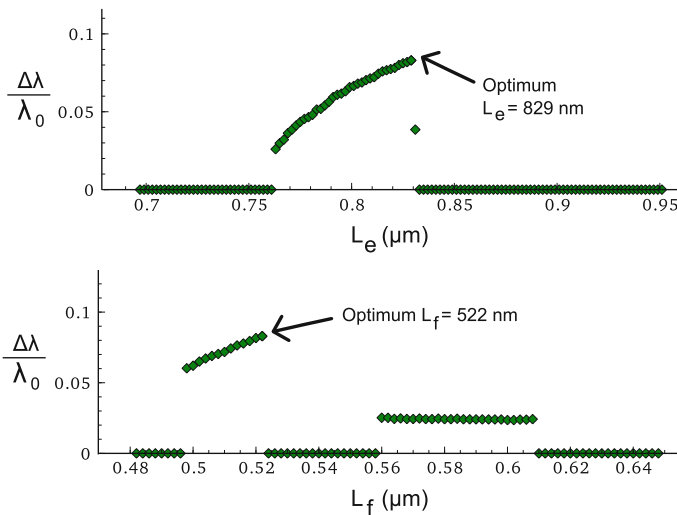
Fig. 2 Evolution of the normalized bandwidth versus the etched length L_e and the filled length L_f. The *arrows* show the optimum values for these parameters which are both at the upper limit of the variation range

from the etching of the slab. The grating thickness can be controlled with more precision during the growth and a selective etching process technique should allow more control on the depth of the etching.

The tolerance measurement of the optimized design has shown large variation range of $\Delta L_e = 68\,\text{nm}$ and $\Delta L_f = 24\,\text{nm}$. However the optimum point is located at a boundary of these variation ranges and the allowed error is of only 2 nm on L_e and even 0 nm on L_f (Fig. 2).

4 Robustness enhancement

In order to increase the tolerance of the design, a more centered point within the variation range should be used. However, during the fabrication process, errors can be made simultaneously on several parameters at a time, especially on L_e and L_f if the period was not well defined during the photolithography step for instance. To complete the tolerance study, the variation ranges of the period $\Lambda = L_e + L_f$ and the fill factor $FF = L_f/\Lambda$ have been evaluated. These extremum values have been plotted on a 2D map in Fig. 3. Thus,
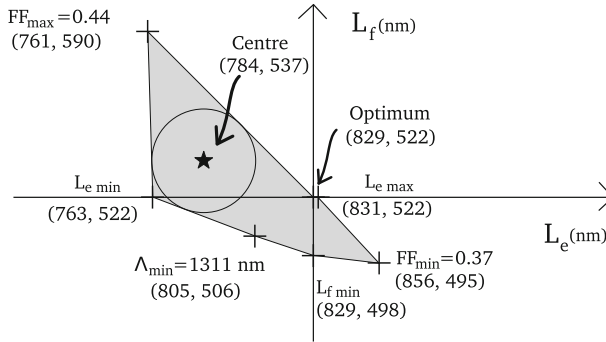
Robust design of Si/Si$_3$N$_4$ HCG mirror

Fig. 3 The tolerance map represents the variation range for the (L_e, L_f) couples while keeping T_g and T_L at their optimum value. The points (+) define a polygon (in *grey*) which vertices correspond to the extrema of the variation range of (L_e, L_f) couples where R_{TM} is below 99.9 % or R_{TE} above 90 % at λ_0 ($\Delta\lambda = 0$ nm). The center of the largest *incircle* of the polygon (⋆) indicates the most tolerant point with respect to the fabrication errors on L_e and L_f

the variation range of L_e, L_f, the period Λ and the fill factor $FF = L_f/\Lambda$ indicates the area of the (L_e, L_f) couples where the previously defined VCSEL requirements are met. The optimum point (829, 522) with the largest bandwidth found by the optimization algorithm is located at the edge of the tolerance area. So, in order to enhance the robustness of the grating with respect to the error of fabrication which could be made on L_e and L_f, a non optimum point located at the centre of the tolerance area has been chosen with $L_e = 784$ nm and $L_f = 537$ nm.

The resulting HCG, which characteristics are summarized in Table 2, exhibits a 186 nm large bandwidth which is 32 nm less than the optimum design reported in Table 1, but is more robust with tolerance values of ±4 % for L_e, ±5 % for L_f and ±2 % for T_g. These values are not as high as the Si/SiO$_2$-based HCG performances which can exhibit 250 nm large bandwidth with up to 10 % of tolerance. These better performances are due to the higher index contrast of the Si/SiO$_2$ system ($n_{SiO2} = 1.509$).

5 Conclusion

In this work, a Si/Si$_3$N$_4$ high contrast grating mirror has been designed and exhibit a 186 nm large 99.9 % high reflectivity bandwidth. The dimension of the mirror structure has been

Table 2 Dimensions and tolerances of the robust mirror

Parameter	Value	Tolerance	Minimum	Maximum
L_e	784 nm	±4 %	735 nm	814 nm
L_f	537 nm	±5 %	512 nm	598 nm
T_g	899 nm	±2 %	882 nm	923 nm
T_L	896 nm	±37 %	566 nm	1,496 nm
$\Delta\lambda$	186 nm			
$\Delta\lambda/\lambda_0$	7 %			

selected by an optimization algorithm which maximizes a quality factor specially defined for a VCSEL application. Then, the tolerances of this optimum design have been evaluated and the robustness with respect to the error of fabrication have been improved by adjusting the grating parameters. This mirror, with a thickness of less than $2\,\mu$m, grooves larger than 500 nm and several percent of tolerance on the grating parameter, should allow laser operation of VCSEL devices at $2.65\,\mu$m.

References

Bachmann, A., Arafin, S., Kashani-Shirazi, K.: New J. Phys. **11**(12), 125014 (2009). http://stacks.iop.org/1367-2630/11/i=12/a=125014

Chevallier, C., Fressengeas, N., Genty, F., Jacquet, J.: Appl. Phys. A Mater. **103**(4), 1139 (2011). doi:10.1007/s00339-010-6059-4

Chevallier, C., Fressengeas, N., Genty, F., Jacquet, J.: Opt. Laser Technol. **44**(3), 626 (2012). doi:10.1016/j.optlastec.2011.09.010. http://www.sciencedirect.com/science/article/pii/S0030399211002672

Debernardi, P., Ostermann, J., Feneberg, M., Jalics, C., Michalzik, R.: . IEEE J. Sel. Top. Quantum Electron. **11**(1), 107 (2005). doi:10.1109/JSTQE.2004.841712

Ducanchez, A., Cerutti, L., Grech, P., Genty, F., Tournié, E.: Electron. Lett. **45**(5), 265 (2009)

Feoktistov, V.: Differential Evolution, Optimization and Its Applications, vol. 5 (Springer US, 2006). doi:10.1007/978-0-387-36896-2_1

Huang, M., Zhou, Y., Chang-Hasnain, C.: Nat. Photon. **1**(2), 119 (2007). doi:10.1038/nphoton.2006.80

Kroshko, D.L.: OpenOpt 0.27 (2009). http://openopt.org/

Mateus, C., Huang, M., Deng, Y., Neureuther, A., Chang-Hasnain, C.: IEEE Photon. Technol. Lett. **16**(2), 518 (2004). doi:10.1109/LPT.2003.821258

Moharam, M.G., Pommet, D.A., Grann, E.B., Gaylord, T.K.: J. Opt. Soc. Am. A **12**(5), 1077 (1995). http://josaa.osa.org/abstract.cfm?URI=josaa-12-5-1077

Rathgen, H.: mrcwa 20080820 (2010). http://mrcwa.sourceforge.net/

Soref, R.A., Emelett, S.J., Buchwald, W.R.: J. Opt. A: Pure Appl. Opt. **8**(10), 840 (2006). http://stacks.iop.org/1464-4258/8/i=10/a=004

Zhou, Y., Huang, M., Chang-Hasnain, C.: IEEE Photon. Technol. Lett. **20**(6), 434 (2008). doi:10.1109/LPT.2008.916969